Preparation and Magnetic Properties of LiCr$_{1-x}$Al$_x$TiO$_4$ (0 ≤ x ≤ 0.4)

M. A. Arillo, M. L. López, M. T. Fernández,* M. L. Veiga, and C. Pico

*Departamento de Química Inorgánica I, Facultad de Ciencias Químicas, Universidad Complutense, 28040-Madrid, Spain; and
Insitut Laue-Langevin, Grenoble, France

Solid solutions LiCr$_{1-x}$Al$_x$TiO$_4$ (0 ≤ x ≤ 0.4) were obtained by solid state reactions in air at 1173 K. Neutron diffraction data have been used to refine the crystal structure of the spinel LiCrTiO$_4$, which is common to all members of the series and shows a cubic symmetry (space group $Fd3m$). Magnetic properties are discussed and the results suggest antiferromagnetic interactions in the octahedral sublattice that provoke an inherent frustration. © 1996 Academic Press, Inc.

INTRODUCTION

The general chemical formula for the spinel-type materials is AB_2O_4. The oxygen ions form a face-centered cubic lattice and the cations occupy interstitial positions; the A cations are located in tetrahedral sites, and the B cations are in octahedral sites. The investigation of cation distribution in spinels, among tetrahedral and octahedral sites, is a suitable method to gain knowledge about the various factors which determine coordination preferences in structural chemistry. Cation site preferences in spinels are well documented (1–3) and some studies (4, 5) have recently emphasized the need for understanding the cation distribution in more complex systems.

Ternary spinels are particularly useful model systems in solid state chemistry, since gradual changes in chemical composition could produce variations in cation distribution which allow the interpretation of physical and chemical properties related to the coordination symmetry of different cations. Such studies are also relevant to the many technological applications of oxide spinels.

In this sense, magnetic properties of compounds possessing a spinel structure show interesting features, mainly ferro- or antiferromagnetism (6, 7). Paramagnetic cations can be distributed on the octahedral or tetrahedral positions and magnetic superexchange interactions in such a structure are strongly dependent on the particular cation arrangement. Thus, interactions between tetrahedral and octahedral sublattices are stronger than those inside the tetrahedral or octahedral sublattices because the angles

and distances between ions are unfavorable for superexchange coupling (8).

This work reports a neutron diffraction refinement for the spinel LiCrTiO$_4$, which allows one to establish a better knowledge of the cation distribution with respect to previous X-ray diffraction results (9, 10). On the other hand, the progressive substitution of a paramagnetic Cr^{3+} ion by diamagnetic Al^{3+} ions introduces changes both in the resulting magnetic behavior and in the cation distribution.

EXPERIMENTAL

Polycrystalline samples of LiCr$_{1-x}$Al$_x$TiO$_4$ were prepared by usual solid state techniques from powdered mixtures of LiNO$_3$, Cr$_2$O$_3$, Al(NO$_3$)$_3$ · 9 H$_2$O, and TiO$_2$ (all reagents supplied by Merck, Germany) in the adequate stoichiometric ratios. Each mixture was preheated in an alumina crucible at 773 K for 5 h to descompose the nitrates and further it was reground and pressed in pellets (at 6 Ton/cm^2). Finally the pellets were heated in air at 1173 K for a day. The process was monitored by X-ray diffraction and single phases were obtained in the compositional range 0 ≤ x ≤ 0.4. For higher x values the upper phase, LiCr$_{0.6}$Al$_{0.4}$TiO$_4$, always appears impurified with LiAl$_5$O$_8$ (11).

X-ray diffraction patterns were recorded with a Philips X'Pert-MPD diffractometer and a 3051/100 goniometer, using Ni filtered Cu$K\alpha$ radiation. A 2θ step size of 0.04° was used. Rietveld's profile analysis method (12) was employed for refinement of X-ray diffraction results in the spinels LiCr$_{1-x}$Al$_x$TiO$_4$.

The neutron powder diffraction data for LiCrTiO$_4$ were collected at room temperature on the high-resolution powder diffractometer D1A at the Institute Laue-Langevin, Grenoble, France. The neutron diffraction pattern was analyzed by the Rietveld's method (12), using the program Fullprof (13).

The magnetic susceptibility measurements were made by using a DSM8 pendulum susceptometer based on the Faraday method. The maximum applied magnetic field was

15 kG with $H(dH/dz) = 29$ kG$^2 \cdot$ cm^{-1}. The equipment was calibrated with Hg(Co(SCN)$_4$) and Gd$_2$(SO$_4$)$_3 \cdot$ 8H$_2$O, being χ independent of the field in the temperature range of measurements. The magnetic susceptibility data have been corrected taking into account the ionic diamagnetic contribution (14).

Chemical analyses were performed by the ICP technique (15) and the results are in good agreement with the proposed stoichiometry.

RESULTS AND DISCUSSION

1. Structural Characterization

The X-ray diffraction patterns for the title phases could be assigned to a cubic symmetry and they were analyzed by the Rietveld method. All the observed reflections could be indexed in the space group $Fd3m$ (No. 227) in which lithium cations were located on the tetrahedral sites ($8a$) and the remaining cations, Cr/Al/Ti, were randomly distributed on the octahedral sites ($16d$). Although this assumption seems to be more reasonable, the corresponding R factors were quite high. In principle, this fact could be due to the low scattering factor for Li as well as the differences between the three cations which would be occupying the same $16d$ sites. Various attempts to improve these reliability values were achieved and better results were obtained (see below). To clarify this uncertainty, neutron diffraction data were recorded for the phase LiCrTiO$_4$. The resulting data for the a unit cell parameter, atomic coordinates, occupation, reliability factors, and unit

TABLE 1

Fractional Atomic Coordinates at 295 K, Crystallographic Data, and Reliability Factors for LiCrTiO$_4$ Obtained by Neutron Diffraction

Atom	Position	X	Y	Z	Occupation	β(Å^2)
Cr	16d	0.5000	0.5000	0.5000	1.000	0.747
Ti	16d	0.5000	0.5000	0.5000	0.882	0.936
Li	16d	0.5000	0.5000	0.5000	0.118	0.936
Ti	8a	0.1250	0.1250	0.1250	0.118	1.105
Li	8a	0.1250	0.1250	0.1250	0.882	1.105
O	32e	0.262(5)	0.262(5)	0.262(5)	1.000	0.482

a (Å) 8.317(3)	V (Å^3) 575.4(7)
R_e 3.86	R_P 4.78
R_{WP} 6.28	R_B 2.76

cell volume are listed in Table 1 and Fig. 1 shows calculated and observed diffraction profiles and the difference between them. Therefore, in the spinel LiCrTiO$_4$ the Cr^{3+} cations seem to occupy half of the $16d$ octahedral coordination sites (occupation factors equal to 1), probably due to its relatively high crystal field stabilization energy (CFSE) in this coordination. On the other hand, there is a random distribution of Li$^+$ and Ti^{4+} cations among the octahedral and tetrahedral sites, their respective CFSE being zero. About 88% of Ti^{4+} are located on octahedral holes whereas about 12% of Li$^+$ cations are placed in these same holes. In the former case it is reasonable to suppose that highly charged formal cations tend to occupy the higher coordina-
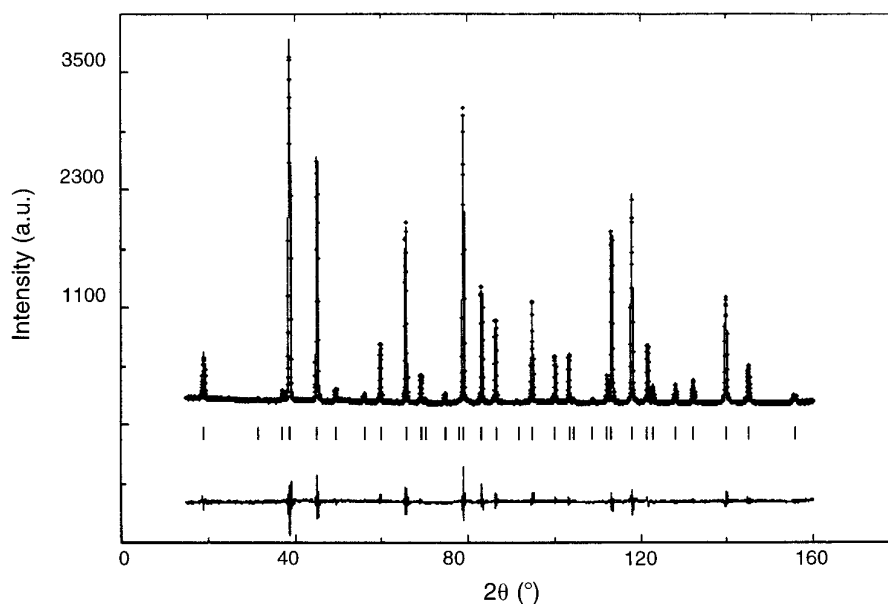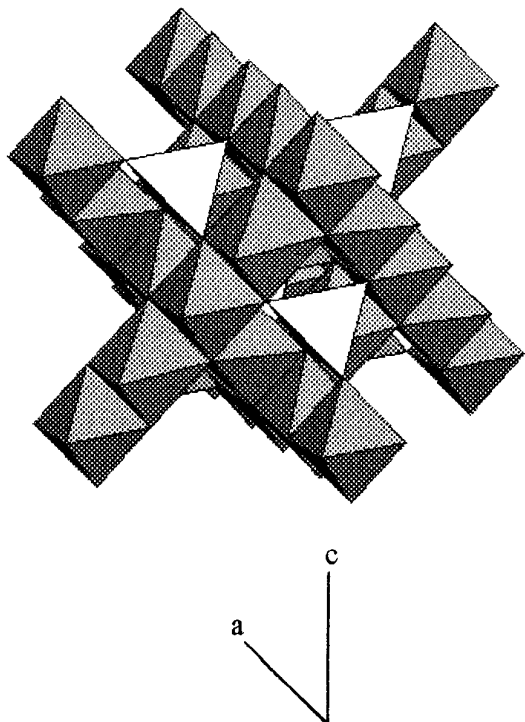

FIG. 1. The observed (...), calculated (—), and difference profiles for LiCrTiO$_4$.

FIG. 2. Structural model of LiCrTiO$_4$.

TABLE 2
Crystallographic Data and Occupation Factors (n_M) for LiCr$_{1-x}$Al$_x$TiO$_4$ (0 ≤ x ≤ 0.4)

	x = 0	x = 0.1	x = 0.2	x = 0.4
a (Å)	8.317(3)	8.320(2)	8.323(4)	8.329(1)
x(O)	0.262(5)	0.260(4)	0.260(1)	0.261(2)
R_B	4.60	5.41	5.93	6.04
R_{WP}	19.3	22.1	17.1	18.8
R_P	13.4	15.3	12.9	14.1
R_e	4.09	3.61	3.69	3.74
$n_{Li}(h_t)^a$	0.882	0.971	0.976	0.989
$n_{Ti}(h_o)^a$	0.882	0.974	0.980	0.992
$n_{Al}(h_o)^b$	—	0.097	0.196	0.397
$n_{Al}(h_t)^b$	—	0.003	0.004	0.003

^{a} $n_M(h_t) + n_M(h_o) = 1$.
^{b} $n_{Al}(h_t) + n_{Al}(h_o) = x$.

tion sites. The introduction of Li$^+$ cations in octahedral sites could be attributed to a relaxation of the local potential energy around highly charged octahedra, which are sharing common edges. A structural model for this material is given in Fig. 2.

The cation distribution obtained from X-ray or neutron diffraction data is shown for comparison in Table 1. We can see a quite good agreement on these results. Therefore, we can admit that the X-ray diffraction results could provide a valid approximation for analyzing the cation distribution for the remaining phases.

The resulting data for all compositions, the a parameter, oxygen coordinate, and reliability and occupation factors, are gathered in Table 2. We can see that the unit cell parameter, a, increases as x does. Nevertheless, taking into account the Shannon ionic radii values for Cr^{3+} (0.615 Å) and for Al^{3+} (0.535 Å) in octahedral coordination, the a values would have to decrease as the Al^{3+} content increases, that is, with x. Having in mind the experimental variation of a, this anomalous behavior could be justified by considering the reticular expansion provoked by the progressive introduction of Ti^{4+} (0.65 Å) in octahedral holes. Within the experimental error there is no change in a between the phases x = 0.0 and x = 0.1, although a significant displacement of Li$^+$ (0.74 Å) from octahedral (12%) to tetrahedral sites is observed.

In this respect, it is interesting to analyze the tendency in the occupation when x increases in the series LiCr$_{1-x}$Al$_x$TiO$_4$ and its relation with the reticular parameters for each one. The Cr^{3+} ions are always located on the same octahedral positions whereas Li$^+$ tends to be displaced toward the tetrahedral sites and, at the same time, Ti^{4+} are progressively shifted to the octahedral sites. The Al^{3+} cations remain mainly located on the 16d sites and are not affected by the x values. From these data we can admit that for the end phase (x = 0.4) there is a near regular distribution of cations and not more than 1% of lithium cations are in octahedral coordination.

On the other hand, these variations in the cation distribution produce an increase in the mean radius for the tetrahedral cations and a diminution for the octahedral ones; both tendencies are practically compensated along the series and thus the unit cell parameters for the different compositions remain nearly constant, although a slight (about 0.15%) and regular increase in a is observed.

Table 3 shows the mean A–O and B–O bond distances, compared with those expected from the sums of Shannon ionic radii, as well as the variation of the unit cell B–B mean distances that can be taken as reference for the parameter variation because both are of the same order, that is 0.14%, for the limit phases.

TABLE 3
Bond Distances (in Å) of LiCr$_{1-x}$Al$_x$TiO$_4$ (0 ≤ x ≤ 0.4)

Composition	B–B	B–O	Shannon r (M)$_o$–O	A–O	Shannon r (M)$_t$–O
0.0	2.941	2.000	2.001	1.943	1.946
0.1	2.942	1.997	1.988	1.951	1.965
0.2	2.943	1.999	1.984	1.959	1.966
0.4	2.945	1.993	1.975	1.965	1.969
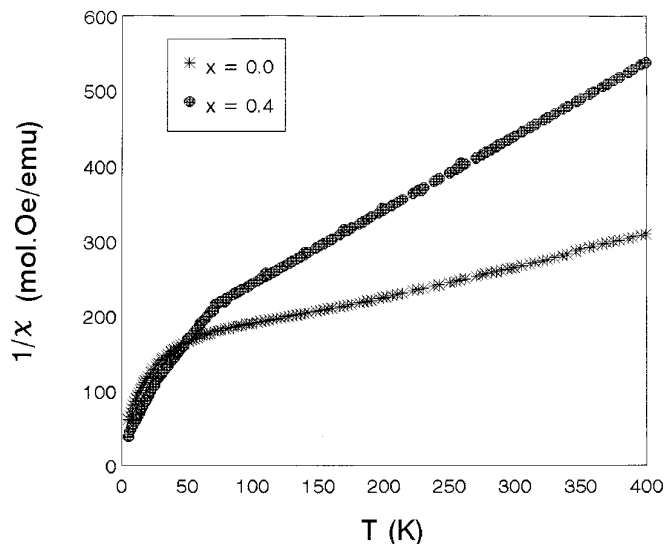
FIG. 3. Temperature dependence of the reciprocal molar susceptibility of $LiCr_{1-x}Al_xTiO_4$.

FIG. 4. Magnetization measurement of $LiCrTiO_4$ as a function of applied field at 77 K.

The remaining members of this series ($x > 0.5$) have been always obtained impurified by some amount of Li-Al_5O_8 and similar trends were registered in all cases, although R factors were poorer than those of the previous phases and they are not included in this structural description. Nevertheless, they are of some interest when we consider the magnetic properties of this system, as we discuss below.

2. Magnetic Properties

From the experimental details given above, the inverse magnetic susceptibility data are plotted in Fig. 3 and the magnetic parameters are gathered in Table 4, for the compositions $x = 0.0$ and 0.4. Assuming a Curie–Weiss model we can deduce for both samples the values of the paramagnetic Curie temperature from the straight lines above 70 K ($\theta = -383$ and -151 K, respectively) and the effective magnetic moment ($\mu_{eff} = 4.53$ and 4.37 μ_B, respectively). These values of μ_{eff} are higher than that expected for the isolated Cr^{3+} free ion, 3.87 μ_B, and this fact could be attributed to ferromagnetic coupling between such paramagnetic
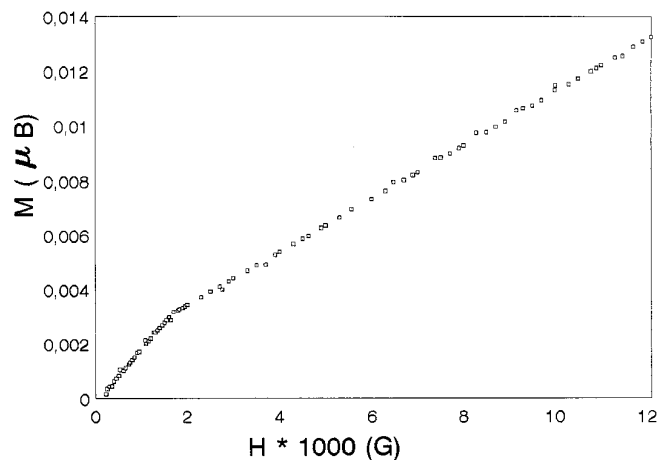
cations, which are located on octahedral sites. This behavior seems to diminish in the sample $x = 0.4$ as a consequence of the introduction of diamagnetic species in the same octahedral coordination giving the composition $[Al_{0.4}Cr_{0.6}]$. Similar results were pointed out for the spinel $LiCrGeO_4$ (4), in which the absence of any long-range magnetic order was attributed to the existence of an analogous disorder in the octahedral sites (Cr and Ge).

In order to analyze this phenomenon, we have carried out magnetization studies (17) at 77 K for the material $LiCrTiO_4$ and the results are given in Fig. 4. Experimental data are fitted to two straight lines which intercept at 2 kG and below this value the observed deviation could also be interpreted on the basis of weak ferromagnetic interactions.

On the other hand, below 70 K there is a marked diminution of μ_{eff} and θ. This behavior seems to be consistent with a model of spin exchange interactions among Cr^{3+} cations giving rise to exchange-coupled dimers, trimers, and higher clusters (10).

However, the absence of any long-range magnetic order in these compounds, as deduced from the absence of a maximum in the $1/\chi$ vs T graph (Fig. 3), is directly related to the existence of disorder in the B sites. As established above there are mainly three kinds of atoms, Cr/Al and Ti, and only one magnetic species, Cr^{3+}, that implies an inherent "frustration" in the B sublattice (17). In this respect, Anderson (18) pointed out that the topology of the octahedral sublattice could not support long-range order through nearest-neighbor exchange interactions alone. The antiferromagnetic B–B interactions would lead to a spin frustration that may also arise from competing nearest-neighbor and next-nearest-neighbor exchange interactions (19, 20) or from the competing interactions of different cations (21).

TABLE 4
Magnetic Parameters of $LiCr_{1-x}Al_xTiO_4$ ($0 \leq x \leq 0.4$)

Composition	T(K)	C(K.emu.mol^{-1})	μ_{eff} (μ_B)	θ
$x = 0$	4.3–20	0.30	1.56	−16
	29–68	1.03	2.87	−119
	70–400	2.56	4.53	−383.2
$x = 0.4$	5.0–25	0.72	2.40	−7.3
	30–69	1.13	3.01	−25.4
	77–400	2.38	4.37	−151

REFERENCES

1. G. Blasse, *Philips Res. Rep. Suppl.* 3 (1964).
2. C. Glidewell, *Inorg. Chim. Acta* **19,** 445 (1976).
3. J. K. Burdett, G. D. Price, and S. L. Price, *J. Am. Chem. Soc.* **104,** 92 (1982).
4. M. Touboul and F. Bourée, *J. Mater. Chem.* **3,** 6 (1993).
5. C. González, M. L. López, M. Gaitán, M. L. Veiga, and C. Pico, *Mater. Res. Bull.* **29** (8), 903 (1994).
6. C. G. Shull, E. O. Wollan, and W. C. Koehler, *Phys. Rev.* **84,** 912 (1951).
7. L. M. Corliss, J. M. Huctings, and F. G. Brockman, *Phys. Rev.* **90,** 1013 (1953).
8. A. H. Morrish, "The Physical Principles of Magnetism." Wiley, New York, 1965.
9. G. Blasse, *J. Inorg. Nucl. Chem.* **25,** 230 (1963).
10. P. M. Lambert, P. P. Edwards, and M. R. Harrison, *J. Solid State Chem.* **89,** 345 (1990).
11. E. Kordes, *Z. Krist. A* **91,** 193 (1935).
12. H. M. Rietveld, *J. Appl. Crystallogr.* **2,** 65 (1969).
13. J. Rodríguez-Carvajal, Program Fullprof, ILL, Grenoble, France, unpublished, 1994.
14. L. N. Mulay and E. A. Boudreaux (Eds.), "Theory and Applications of Molecular Paramagnetism," p. 494. Wiley, New York, 1976.
15. S. Geenfield, I. L. L. Jones, and C. T. Berry, *Analyst* (*London*) **89,** 713 (1964).
16. J. G. Lee, K. V. Ramanujachary, and M. Greenblatt, *J. Solid State Chem.* **118,** 292 (1995).
17. D. Fiorani, L. Gastaldi, A. Lapiccirella, S. Viticolo, and N. Tomassini, *Solid State Commun.* **32,** 831 (1979).
18. P. W. Anderson, *Phys. Rev.* **102,** 1008 (1956).
19. J. Villian, *Z. Phys. B* **33,** 31 (1979).
20. M. Alba, J. Hammann, and M. Nogues, *J. Phys. C* **15,** 5441 (1982).
21. D. Fiorani, M. Nogues, and S. Viticolo, *Solid State Commun.* **41,** 537 (1982).